# Prototype Filter for QAM-FBMC Systems Based on Discrete Prolate Spheroidal Sequences (DPSS)

Iandra Galdino, Rostom Zakaria, Didier Le Ruyet, Marcello de Campos

IEEE Access
Multidisciplinary | Rapid Review | Open Access Journal

Received January 19, 2022, accepted February 23, 2022, date of publication March 8, 2022, date of current version March 24, 2022.

*Digital Object Identifier 10.1109/ACCESS.2022.3157304*

# Prototype Filter for QAM-FBMC Systems Based on Discrete Prolate Spheroidal Sequences (DPSS)

**IANDRA GALDINO[1], ROSTOM ZAKARIA[2], DIDIER LE RUYET[2], (Senior Member, IEEE), AND MARCELLO L. R. DE CAMPOS[3], (Senior Member, IEEE)**

[1]Department of Computer Science, Fluminense Federal University (UFF), Niterói 24210-240, Brazil
[2]CEDRIC/LAETITIA Laboratory, Conservatoire National des Arts et Métiers, 75003 Paris, France
[3]Electrical Engineering Program, COPPE, Federal University of Rio de Janeiro, Rio de Janeiro 21941-914, Brazil

Corresponding author: Iandra Galdino (iandra.galdino@smt.ufrj.br)

This work was supported in part by the Coordenação de Aperfeiçoamento de Pessoal de Nível Superior—Brasil (CAPES) under Finance Code 001.

**ABSTRACT** In conventional wireless communications, cyclic-prefix orthogonal frequency division multiplexing (CP-OFDM) has been adopted as the baseline multicarrier scheme. Despite their corroborated merits, they are explored only in the asynchronous and strictly orthogonal scenario. To overcome the limitations observed in CP-OFDM, to support the constraints imposed by different 5G scenarios, and also to improve robustness against channel impairments, several waveforms have been investigated. Quadrature amplitude modulation associated with filter-bank multicarrier (QAM-FBMC) has been an auspicious technology for 5G communication systems and beyond. The main feature of QAM-FBMC is its capacity for high spectral confinement, which is possible thanks to the per-subcarrier filtering. Aiming to improve the QAM-FBMC performance, in this paper, we propose a prototype filter design based on the discrete prolate spheroidal sequences (DPSS), also known as Slepian sequences. The presented filters were obtained by optimizing the weights that are used to compose the desired prototype filter to such an extent that they minimize the intrinsic interference of the system. At the same time, these weights keep spectral confinement of the filter for a previously determined bandwidth limitation. Simulation results show that the optimized filters achieve higher intrinsic interference attenuation than the competitors. Indeed, we can confirm the improvement in the system performance brought by the usage of the optimized filters through the bit error rate (BER) evaluation. Furthermore, the proposed method is flexible thanks to the suitability of its parameters.

**INDEX TERMS** Filter-bank multicarrier, QAM-FBMC, wireless communication, 5G, prototype filter deign, DPSS, Slepian functions.

## I. INTRODUCTION

Waveform design for post orthogonal-frequency-division-multiplexing (OFDM) systems, *e.g.*, the fifth generation (5G) and beyond (B5G), is a challenge due to the amount and the nature of the services that must be provided [1]–[3]. Among the recent candidates we can cite the offset-quadrature amplitude modulation filter-bank multicarrier (OQAM-FBMC) [4], [5]. Its major characteristics lie in keeping only the real part of the orthogonality condition, crucial for OFDM systems, and in using a per-subcarrier pulse-shaping to reduce out-of-band emissions (OOBE). Consequently, it provides flexibility in waveform design when compared to OFDM and allows heterogeneous services, which is also a requirement of 5G/B5G communication systems. Unfortunately, the one-dimensional intrinsic interference observed in OQAM-FBMC systems becomes a source of problems when combining known techniques, like multiple-input multiple-output (MIMO) and maximum likelihood (ML) detection [6], [7].

Pulse-shaping OFDM systems with good time-frequency localization (TFL) have been proposed in [8], [9] to cope with doubly-selective channels. In order to keep the perfect reconstruction of the data, the authors in [10], [11] have considered a time-frequency lattice associated with an OFDM system with a lattice density $(1/TF)$ lower than 1 (*i.e.* $TF > 1$), where $T$ is the symbol period and $F$ is the subcarrier frequency spacing. To overcome the drawbacks observed in OQAM-FBMC, a QAM-based FBMC scheme (QAM-FBMC) with a single prototype filter has been

The associate editor coordinating the review of this manuscript and approving it for publication was Haipeng Yao.

proposed in [12]. It can be seen as a generalized OFDM with a time-frequency lattice of density equal to one. A more complex structure of QAM-FBMC, composed of two prototype filters, has been proposed and studied in [13] and [14]. An even more complex structure, based on several prototype filters, was proposed in [15]. The use of more than one prototype filter reduces the interference but requires more elaborated receivers in order to mitigate the observed residual intrinsic interference.

Several researchers have been working on different techniques for enhancing QAM-FBMC performance. A basic iterative interference estimation and cancellation have been proposed in [16]. The authors in [17] proposed an interference mitigation scheme based on precoding and decision feedback equalization. In [18] researchers proposed an iterative interference cancelation (IIC) receiver to minimize the interference. Also, the authors of [19] proposed a nonlinear receiver, that uses IIC and parallel interference cancellation (PIC) concepts in multiple-input multiple-output (MIMO) systems with minimum mean square error (MMSE) receiver.

We can also find in the literature several works on prototype filter design for QAM-FBMC systems in an attempt to enhance its performance. In [13] the authors proposed the prototype filter called Type I, which is based on the minimization of the self inter-symbol interference (ISI) subjected to the fall-off-rate limitation. As the obtained filter in [13] was poorly concentrated in the time-domain, another waveform design considering time domain localization based on a single prototype filter was suggested in [20] at a cost of a slight increase in interference. In [20] the real coefficients were obtained from the minimization of self signal-to-interference ratio (self-SIR), under the constraints of fall-off rate and time dispersion. By using a global optimization algorithm, the authors proposed three different filters. The number of frequency-domain coefficients of their filters was set as 7, 11, and 15, which led to the filters named Case A, Case B, and Case C, respectively. We can also cite filter design proposals based on carrier frequency offset (CFO) [21]; filter design proposals specifically for minimum mean square error (MMSE) based receiver for a given signal-to-noise rate (SNR) value [22]; and, more recently, a design based on the ISI minimization subject to OOBE limitation [23]. However, the performance evaluations of these prototype filters remain unsatisfactory, since each proposal considers different parameters for the optimization, such as specific SNR, bandwidth, or class of the receiver. Consequently, a direct comparison of their performances is questionable.

The authors of [13] have proposed the use of two prototype filters to reduce interference. However, the bandwidth of the second filter is significantly larger than that of the first filter. This change makes the comparison to the case of using one prototype filter unfair. Besides, the complexity of the system also increases.

We can look at prolate spheroidal wave functions (PSWFs) proposed by Slepian [24], [25], as a possible solution for QAM-FBMC prototype filter design. David Slepian proposed a solution for the time and frequency localization through a set of functions denominated prolate spheroidal wave functions (PSWFs), which are maximally energy concentrated in a given time and bandwidth limitation. It is known that the Slepian solution for the discrete-time problem, called discrete prolate spheroidal sequences (DPSS), is the equivalent version of PSWFs in discrete-time domain [26], consequently they have the same properties. Both DPSS and PSWFs have been widely studied [27]–[31].

The DPSS has a wide range of classical signal processing applications [32]–[38]. Compressive sensing [33], parametric waveform and detection of extended targets [34], wall clutter mitigation and target detection [35], design of baseband receivers [36], fiber Bragg grating (FBG) sensors for optical sensing systems [37], and multipath suppression for continuous waves [38] are just few examples.

We propose, in this paper, a prototype filter specifically designed for QAM-FBMC systems considering a matched filter at the receiver. We consider the discrete prolate spheroidal sequences (DPSS) in order to achieve good energy concentration for a given time and bandwidth limitation. However, differently from traditional filter designs, we did not minimize the OOBE, but the intrinsic interference of the system. We compare the performance of the obtained filters to some known filters from the state of the art.

The proposed prototype filters show high interference attenuation and, as expected, significantly improve the system BER performance. In addition, since the bandwidth of the desired filter is adjustable through the DPSS parameters, the proposed procedure shows flexibility in terms of spectrum confinement.

The contributions presented in this paper are:

- A new prototype filter for FBMC-QAM based on the most energy concentrated DPSS sequences.
- A new technique to optimize prototype filters for QAM-FBMC based on DPSS that minimize the intrinsic interference for a given bandwidth limitation.
- A system performance comparison of the proposed prototype filters with the ones in the literature considering both AWGN and fading channels.

For the sake of clarity, we start by describing the QAM-FBMC system and deriving its intrinsic interference in Section II. Then, we give an overview of PSWF and DPSS in Section III. We present our DPSS-based prototype filter design as an optimization problem in Section IV. The optimization results are presented in Section V and the performance evaluation of the proposed filters in Section VI. The conclusions are drawn in Section VII.

## II. SYSTEM MODEL OF QAM-FBMC

Let us define $a_{k',n'}$ as the transmitted symbol allocated at the $k'$-th subcarrier and transmitted in the $n'$-th QAM-FBMC symbol. Thus, the QAM-FBMC transmitted signal, also known as the Weyl–Heisenberg system of functions [39],

can be given by

$$s(t) = \sum_{n'} \sum_{k'=0}^{M-1} a_{k',n'} g(t - n'T) e^{j2\pi Fk't}, \tag{1}$$

where $M$ is the number of subchannels, $g(t)$ is the unit-energy prototype filter with overlapping factor $K$ (*i.e.* length $L_g = KM$), $T$ is the symbol time, and $F$ is the subcarrier frequency spacing.

Considering additive white Gaussian noise channel (AWGN), the continuous-time received signal can be described as

$$r(t) = s(t) + v(t), \tag{2}$$

where $v(t)$ is Gaussian white noise.

At the receiver, the output of the $n$-th symbol of the $k$-th filter can be expressed as

$$\begin{aligned}
&\tilde{a}_{k,n} \\
&= \int_{-\infty}^{\infty} r(t) g^*(t - nT) e^{-j2\pi Fkt} dt \\
&= \int_{-\infty}^{\infty} \Big( \sum_{n'} \sum_{k'=0}^{M-1} a_{k',n'} g(t - n'T) e^{j2\pi Fk't} \Big) \\
&\quad g^*(t - nT) e^{-j2\pi Fkt} dt + v_{k,n} \\
&= \sum_{n'} \sum_{k'=0}^{M-1} a_{k',n'} \int_{-\infty}^{\infty} g(t - n'T) \\
&\quad g^*(t - nT) e^{-j2\pi F(k-k')t} dt + v_{k,n} \\
&= a_{k,n} + v_{k,n} \\
&\quad + \underbrace{\sum_{\substack{(k',n') \\ \neq \\ (k,n)}} a_{k',n'} \int_{-\infty}^{\infty} g(t - n'T) g^*(t - nT) e^{-j2\pi F(k-k')t} dt}_{\text{interference}},
\end{aligned} \tag{3}$$

where $v_{k,n} = \int_{-\infty}^{\infty} v(t) g^*(t - nT) e^{-j2\pi Fkt} \mathrm{d}t$.

Let us recall the ambiguity function definition [40]

$$A_g(T_0, F_0) = \int_{-\infty}^{+\infty} g(t) g^*(t - T_0) e^{-j2\pi F_0 t} dt, \tag{4}$$

where $^*$ denotes complex conjugate. By setting $\Delta_n = (n - n')$ and $\Delta_k = (k - k')$ we can derive the function $A_g(T\Delta_n, F\Delta_k)$ as

$$A_g(\Delta_n T, \Delta_k F) = \int_{-\infty}^{+\infty} g(t - n'T) g^*(t - nT) e^{-j2\pi \Delta_k Ft} dt. \tag{5}$$

Thus, by using (5) we can rewrite (3) as

$$\tilde{a}_{k,n} = a_{k,n} + \underbrace{\sum_{(k',n') \neq (k,n)} a_{k',n'} A_g(\Delta_n T, \Delta_k F)}_{\text{interference}} + v_{k,n}. \tag{6}$$

As an example, we show in Fig. 1 the ambiguity function of the prototype filter case C proposed in [20] for QAM-FBMC systems with a single filter. The red marks represent the rectangular lattice structure of the QAM-FBMC system. These points, except for the one in the center ($(\Delta_k, \Delta_n) = (0, 0)$), indicate where we should sample the ambiguity function in order to obtain the intrinsic interference coefficients which will be used to compute the system interference.

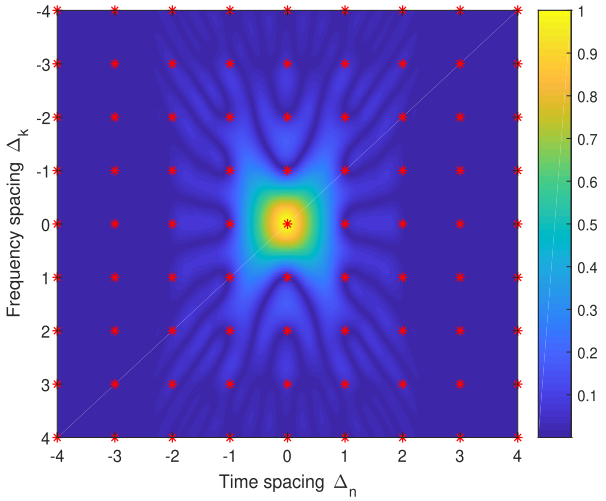


**FIGURE 1.** Magnitude of ambiguity function for Case C prototype filter [20], ($|A_g(T, F)|$).

Let us define the intrinsic interference coefficients as $\Gamma_{\Delta_n,\Delta_k} = A_g(\Delta_n T, \Delta_k F)$, represented by the red points in Fig. 1. Therefore, the total interference over the $k$-th subcarrier at the $n$-th time instant can be calculated using the interference coefficients to weight the neighbor symbols as follows

$$I_{k,n} = \sum_{(k',n') \neq (k,n)} a_{k',n'} \Gamma_{\Delta_k \Delta_n}. \tag{7}$$

As we can see, these coefficients are essential to calculate the intrinsic interference, since the quantity of $\Gamma_{\Delta_k,\Delta_n}$, when $(k', n') \neq (k, n)$, is dedicated to the interference that comes from the surrounding symbols $(k', n')$.

## III. DISCRETE PROLATE SPHEROIDAL SEQUENCES (DPSS)

The problem of confining a signal in time and frequency domains simultaneously has been discussed in digital signal communication systems for a long time [41]. The energy time-concentration level of a signal can be measured as the fraction of the signal's energy lying in a time interval of length $2T_0$. This measure can be mathematically written as

$$\mathrm{P} = \frac{\int_{-T_0}^{T_0} |g(t)|^2 \mathrm{d}t}{\int_{-\infty}^{+\infty} |g(t)|^2 \mathrm{d}t}. \tag{8}$$

If $g(t)$ is strictly time-limited to the interval $[-T_0, T_0]$ the energy concentration level P will achieve its maximum value of one. As time and frequency are inversely related, the Fourier transform of a time-limited function is equal to an infinitely wide bandwidth.

The time and frequency concentration issue, which consists in maximizing P while keeping $g(t)$ band-limited, was first studied by Slepian, Pollak, and Lindau [24], [25]. They developed a set of band limited functions $\psi_p(t, b)$ that are maximally concentrated in a given time interval [24]. These functions are called Prolate Spheroidal Wave Functions (PSWFs), also known as Slepian functions.

The approach used by Slepian is based on angular and radial solutions in spheroidal coordinates of the first kind to the Helmholtz wave equation $S_{0_p}(b, t)$ and $R_{0_p}(b, 1)$, respectively. Hence, the PSWFs can be expressed as [24], [42]

$$\psi_p(t, b) = \frac{\sqrt{\lambda_p(b)/T_0}}{\sqrt{\int_{-1}^{1} \left(S_{0_p}(b, t)\right)^2 \mathrm{d}t}} S_{0_p}\left(b, \frac{t}{T_0}\right), \tag{9}$$

where $\lambda_p(b)$ is given by

$$\lambda_p(b) = \frac{2b}{\pi}\left[R_{0_p}(b, 1)^2\right]. \tag{10}$$

The PSWFs are dependent on the continuous time parameter $t$, on the order $p$ of the function, on the time parameter $T_0$, and also on the parameter $b$ which is defined as

$$b = \frac{T_0 B}{2}, \tag{11}$$

where $B$ is the bandwidth of $\psi_p(t, b)$ of a given order $p$.

The PSWFs, $\psi_p(t, b)$, concentrated in the interval $[-T_0, T_0]$, can be defined as the normalized eigenfunctions of the following integral equation [26], [27]:

$$\int_{-T_0}^{T_0} \frac{\sin(\pi(x - t)B)}{\pi(x - t)} \psi_p(t, b)\mathrm{d}t = \lambda_p(b)\psi_p(x, b). \tag{12}$$

The sinc function in (12) can be regarded as a symmetric Toeplitz operator kernel, and the integral of $\psi_p(t, b)$ multiplied by this kernel can be called a symmetric Toeplitz operator [26]. Also, $\lambda_p(b)$ are the eigenvalues of the sinc function kernel, which can also be seen as the index of energy concentration on the interval $[-T_0, T_0]$ [43]. If $\lambda_0(b)$ denotes the largest eigenvalue of (12), then its corresponding eigenfunction, $\psi_0(t, b)$, is commonly called Slepian window, or prolate spheroidal window in the continuous-time domain.

In addition, we can also examine the time/frequency concentration problem in discrete time. For a given time interval $2T_0$ with $L$ samples, and for each $p = 0, 1, 2, \ldots, L - 1$, Slepian defined the discrete Prolate Spheroidal Sequences (DPSS) $\left(\phi_c^{(p)}(L, B)\right)$ as the real solution to the system of equations

$$\sum_{l=0}^{L-1} \frac{\sin(\pi(c - l)B)}{\pi(c - l)} \phi_l^{(p)}(L, B) = \lambda_p(L, B)\phi_c^{(p)}(L, B) \tag{13}$$

for $c \in \mathbb{Z}$, and $\lambda_p(L, B)$ are the eigenvalues of the sinc function kernel [44]. This is the discrete time representation of the system described in (12).

In our application, we are interested in the sequences $\phi_c^{(p)}(L, B)$ limited to $c \in \{0, L - 1\}$, obtained by index-limiting the DPSS. In this case, the sequence $\boldsymbol{\phi}^{(0)}(L, B)$ is the unique sequence that is time-limited and the most frequency-concentrated, $\boldsymbol{\phi}^{(1)}(L, B)$ is the second sequence having maximum energy concentration among the DPSS, and orthogonal to $\boldsymbol{\phi}^{(0)}(L, B)$, and so on. Therefore, we can rewrite (13) in a matrix approach as

$$Q(L, B)\boldsymbol{\phi}^{(p)}(L, B) = \lambda(L, B)\boldsymbol{\phi}^{(p)}(L, B). \tag{14}$$

These sequences are thus seen to be the eigenvectors of the $L \times L$ matrix $Q(L, B)$ with elements [44], [45]:

$$Q(L, B)_{l,c} = \frac{\sin(\pi(l - c)B)}{\pi(l - c)} \quad l, c = 0, 1, 2, \ldots, L - 1 \tag{15}$$

In Fig. 2 we illustrate some of these sequences.

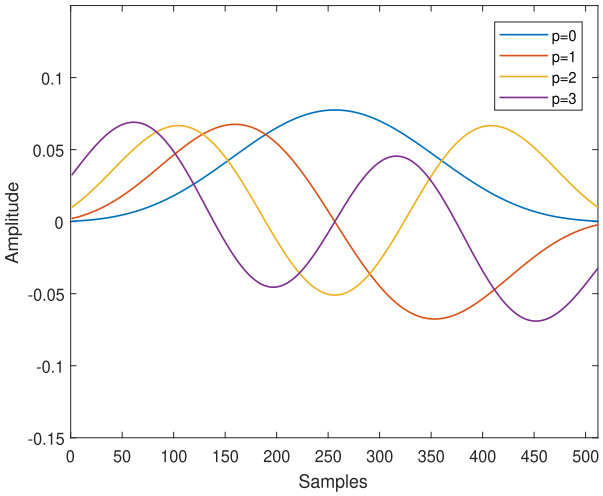


**FIGURE 2. Example of discrete prolate spheroidal sequences (DPSS) of length $L = 512$.**

PSWFs should not be confused with the solution of the discrete-time energy concentration problem, the DPSS. DPSS are much simpler to calculate, and they are known only in a finite interval [27].

## IV. DPSS-BASED PROTOTYPE FILTER DESIGN

The features presented here suggest the potential utility of DPSS for filter-bank multicarrier systems. The first prolate sequence, $\boldsymbol{\phi}^{(0)}(L, B)$, is also known as the classical prolate window. It provides the optimum frequency-concentrated pulse for a given filter length and bandwidth [44]. It is defined as the eigenvector corresponding to the largest eigenvalue of the matrix $Q(L, B)$, usually called Slepian window, or prolate spheroidal window in the discrete-time domain.

Another possible solution that we can think of for filter design is the Kaiser window [46], [47], which employs Bessel functions in order to obtain an approximation of the prolate window. Although it has the advantage of its formulation through a closed-form expression, it is sub-optimal in terms of out-of-band leakage when compared to the prolate window.

Knowing favorable characteristics of discrete prolate spheroidal sequences, we propose a prototype filter design

technique based on DPSS, and we optimize the obtained filter. For this, we consider the spectral confinement, through the band-time parameter of DPSS, and minimize the intrinsic interference of the QAM-FBMC system by using its ambiguity function. We start by designing a function that represents the desired prototype filter using the DPSS.

As the eigenvalues can be regarded as the index of energy concentration of the DPSS [24], our proposal consists in selecting the eigenvectors $\boldsymbol{\phi}^{(p)}(L_g, B)$ of matrix $Q(L_g, B)$ whose eigenvalues $\lambda_p(L_g, B)$ are higher than a certain threshold $\gamma$. The first eigenvalues have strong energy-concentration behavior, they are very close to 1, and the remaining eigenvalues are close to 0 [24]. By doing this process, we select the $N_e$ most energy concentrated sequences $\boldsymbol{\phi}^{(p)}(L_g, B)$ for a given band limitation $B$.

Finally, the proposed prototype filter can be described as a weighted sum of the $N_e$ sequences as follows:

$$\boldsymbol{g} = \sum_{p=0}^{N_e-1} w_p \boldsymbol{\phi}^{(p)}(L_g, B), \tag{16}$$

where $\boldsymbol{g} = \left[g[0], g[1], \ldots, g[L_g - 1]\right]$ is the discrete response of $g(t)$ with $g[m] = g\left(m\frac{T}{M}\right)$, and $w_p$ is the weight coefficient.

From the definition of the desired prototype filter given in (16), and taking into account the interference of the system described in (7), we propose an optimization problem to find the best prototype filter for QAM-FBMC systems. In this sense, we want to find the optimal weights $w_p$ of the prototype filter that minimize the energy of the intrinsic interference coefficients $\Gamma_{\Delta_k \Delta_n}$ subject to the filter energy constraint. So that, we formulate our optimization problem as

$$\begin{aligned} \min_{\boldsymbol{\omega}} \quad & \sum_{\substack{(k',n') \\ \neq \\ (k,n)}} \left| \sum_m g[m - n'M] g^*[m - nM] e^{-j\frac{2\pi \Delta_k m}{M}} \right|^2 \\ \text{s.t.} \quad & \boldsymbol{g}^{\mathrm{H}} \boldsymbol{g} = 1 \end{aligned} \tag{17}$$

where the cost function is the discrete version of the ambiguity function given in (5).

In order to solve the above optimization problem, we use in this work the interior point (IP) method [48]. We have done the optimization several times, each time with different random initial weights $\boldsymbol{w}$, and we select the best-obtained result, *i.e.* the one with the smallest amount of interference. Our obtained prototype filters are denoted as DPSS-based filters (DPSSb).

Algorithm (1) describes the procedure adopted to solve the optimization problem (17).

**Algorithm 1** Prototype Filter Design.

**procedure** Filter Design($L_g$, $B$, $i_{max}$)
  $\text{interf}_{min} \leftarrow \infty$
  compute $\mathbf{Q}(L_g, B)$ as in (15)
  select the eigenvalues greater than $\gamma$
  select the corresponding eigenvectors $\boldsymbol{\phi}^{(p)}(L_g, B)$
  **for** $i = 1$ to $i_{max}$ **do**
    $\boldsymbol{w} \sim \mathcal{CN}(\mathbf{0}_{N_e \times 1}, \boldsymbol{I}_{N_e})$
    $\boldsymbol{w} \leftarrow \boldsymbol{w}/\|\boldsymbol{w}\|$
    compute $g$ according to (16)
    $\boldsymbol{w} \leftarrow$ solution of problem (17) through IP
    compute $\boldsymbol{g}$ according to (16)
    $\text{interf} = \sum_{(k',n') \neq (k,n)} |\Gamma_{\Delta_k \Delta_n}|^2$
    **if** interf $<$ $\text{interf}_{min}$ **then**
      $\text{interf}_{min} \leftarrow$ interf
      $\boldsymbol{g}_{opt} \leftarrow \boldsymbol{g}$
    **end if**
  **end for**
  **return** $\boldsymbol{g}_{opt}$
**end procedure**

## V. OPTIMIZATION RESULTS

In this section, we present the obtained optimization results for a specific FBMC-QAM system settings. We set the overlapping factor of the desired filter as $K = 4$, and the number of subcarriers $M = 128$, which results in a filter length $L_g = 512$.

For a good compromise between $N_e$ and OOBE, we used in our designs the threshold $\gamma = 0.99$ for the eigenvalues. For a fair comparison to the state-of-the-art filters known in the literature, we have determined the bandwidth as $B = 7/M$ for the optimization of the filter that was compared to the Case C filter proposed in [20]. For the comparison to the Type I filter proposed in [13] we set the bandwidth $B = 1.7/M$. The compared filters have approximately the same bandwidth. These filters have been chosen due to their characteristics, they were not optimized for a specific SNR or CFO. To the best of our knowledge, there is no prototype filter in the literature for QAM-FBMC with bandwidth $B = 3/M$, but we have also optimized a prototype filter with this bandwidth in order to demonstrate the proposed procedure flexibility.

In the case of $B = 1.7/M$, by setting $\gamma = 0.99$, we have found $N_e = 3$ eigenvectors, therefore we had to optimize 3 weights $w_p$. In Fig. 3 we present the ambiguity function of the DPSS-based optimized filter. As we can notice, the interference spreads differently in time and frequency domains. It spreads more in time than in the frequency domain.

We have also compared the frequency response of the optimized DPSSb $B = 1.7/M$ filter with the frequency response of Type I filter [13] in Fig. 4, both of them normalized to unit energy. As expected, due to the choice of $B$, they have approximately the same bandwidth. However, their energy distribution is not the same. It happens due to the filter design procedure, which is focused on the intrinsic interference minimization, not in OOBE, as observed in classical filter designs.

The optimization procedure was also applied for the comparison with the Case C filter [20]. We present in Fig. 5 the ambiguity function of the optimized DPSSb $B = 7/M$ filter.

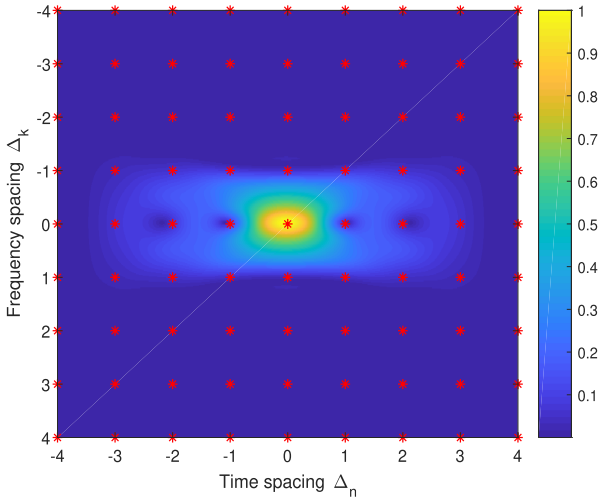


**FIGURE 3.** Magnitude ambiguity function of the proposed DPSSb 1.7/*M* filter, ($|A_g(T, F)|$).

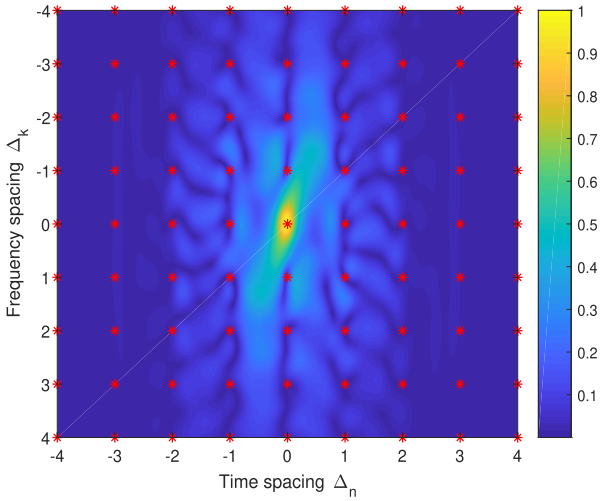


**FIGURE 5.** Magnitude ambiguity function of the proposed DPSSb filter 7/*M*, ($|A_g(T, F)|$).

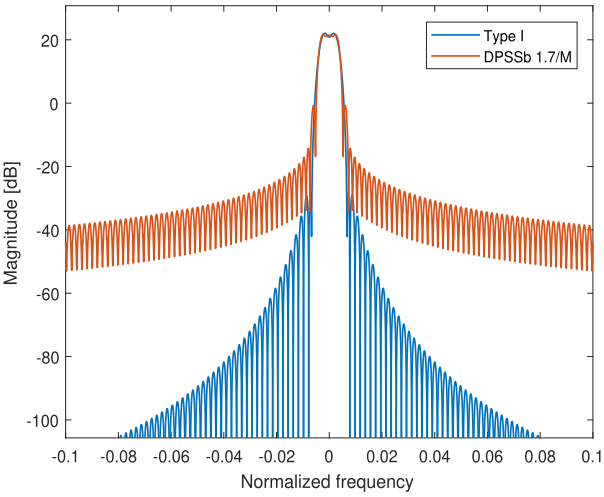


**FIGURE 4.** Magnitude frequency response of the proposed DPSSb 1.7/*M* filter and Type I filter [13].

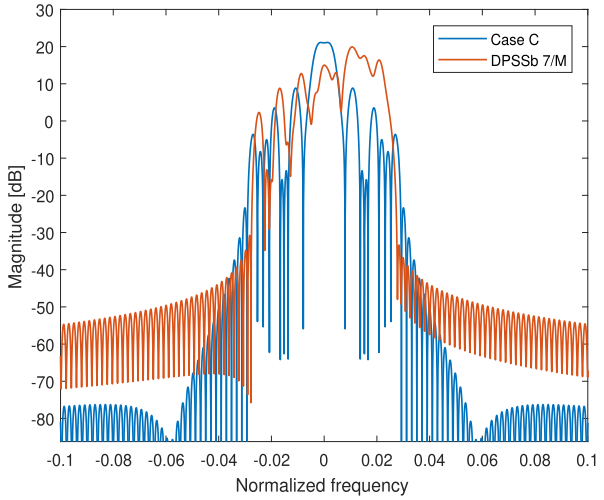


**FIGURE 6.** Magnitude frequency response of the proposed DPSSb filter and Case C [20].

For this optimization, considering $\gamma = 0.99$, the number of selected eigenvectors was $N_e = 25$.

The ambiguity function of the DPSS-based $7/M$ optimized filter is not symmetric. This fact comes from the complex values of the optimized weights. As expected, comparing this ambiguity function to that for $B = 1.7/M$, we can notice an increase in the interference spreading in the frequency domain. It comes from the fact that, in this case, we are optimizing a filter with bandwidth far greater than the subcarrier spacing $1/M$.

The comparison between the frequency response of DPSSb $7/M$ filter and Case C [20] filter is also presented in Fig. 6. Once again, the optimized filter and the known filter have approximately the same bandwidth, however, their energy distribution is not the same.

Despite achieving higher attenuation at the edges of the transmission band, the passband of the DPSSb $7/M$ is not flat. This result comes from the fact that the bandwidth of DPSSb $7/M$ comprises more than one subcarrier spacing ($1/M$). As we minimize the interference coefficients $\Gamma_{\Delta_k \Delta_n}$, which are spaced by one subcarrier spacing, some of them are inside the considered passband of the optimized filter.

In order to make a comparison of the prototype filters, we present, in Table 1, some characteristics of the known and the proposed filters. We compare the inter-symbol interference (ISI) observed in a QAM-FBMC system when using all of these prototype filters. Besides, we evaluate the out-of-band energy (OOBE) of them considering their bandwidth and we also classify them by the nature of their coefficients.

By increasing the desired bandwidth it is possible to decrease the ISI of the optimized prototype filter. Despite having approximately the same bandwidth, the DPSSb $1.7/M$ filter presents smaller ISI than the Type I filter, however, it happens at a cost of higher OOBE. Unlike what happens

**TABLE 1. ISI and OOBE of different filters.**

| Filter | ISI | Coefficient | OOBE |
|---|---|---|---|
| Case C [20] | -17.42 dB | Real | 5.28e-04 |
| DPSSb (proposed) 7/M | -18.95 dB | Complex | 4.21e-06 |
| DPSSb (proposed) 3/M | -14.47 dB | Complex | 3.30e-05 |
| Type I [13] | -10.63 dB | Complex | 4.68e-06 |
| DPSSb (proposed) 1.7/M | -12.60 dB | Complex | 3.54e-04 |

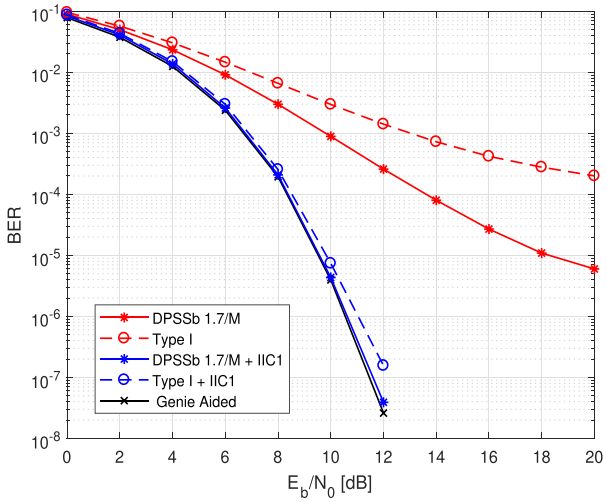


**FIGURE 7. BER performance of QAM-FBMC system with 4QAM modulation, DPSSb 1.7/*M* filter and Type I [13] filter over AWGN channel.**

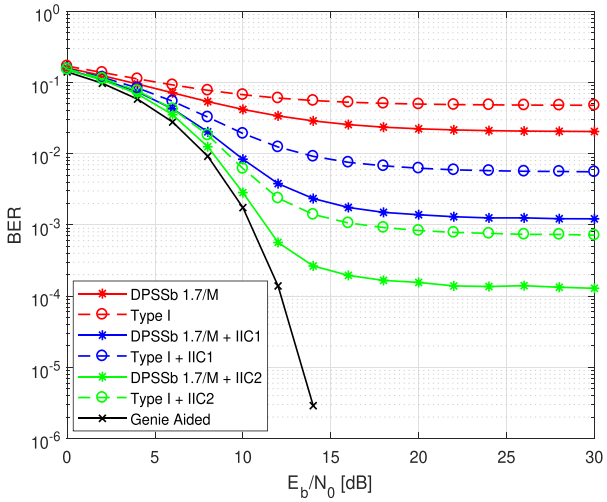


**FIGURE 8. BER performance of QAM-FBMC system with 16QAM modulation, DPSSb 1.7/*M* filter and Type I [13] filter over AWGN channel.**

with the DPSSb 1.7/$M$ filter, the optimized DPSSb 7/$M$ has approximately the same bandwidth as that of the Case C filter. Its ISI is smaller and also its OOBE. This fact can be explained by the complex nature of the optimized filter coefficients, whereas Case C filter coefficients are real. It is important to point out that the proposed DPSSb 7/$M$ filter achieves the highest interference attenuation among the optimized filters, and the smallest OOBE.

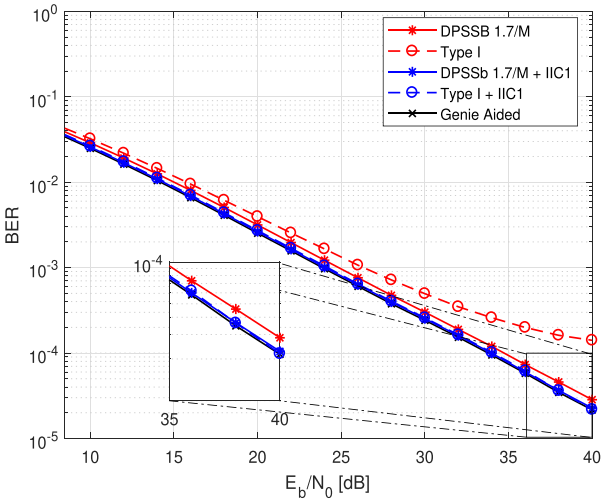


**FIGURE 9. BER performance of QAM-FBMC system with 4QAM modulation, DPSSb 1.7/*M* filter and Type I [13] filter over pedestrian channel.**

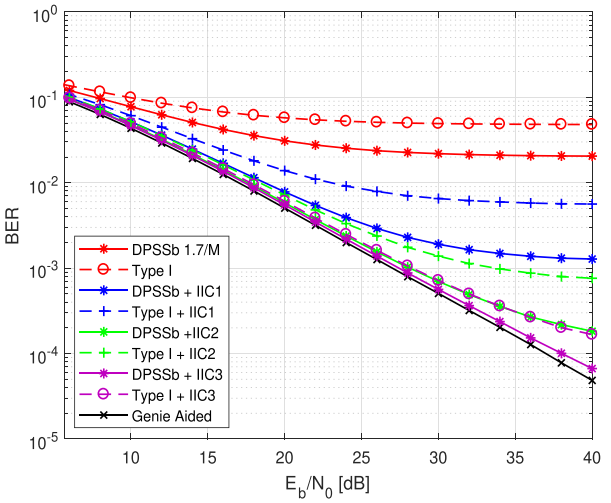


**FIGURE 10. BER performance of QAM-FBMC system with 16QAM modulation, DPSSb 1.7/*M* filter and Type I [13] filter over pedestrian channel.**

## VI. PERFORMANCE EVALUATION

In this section we evaluate the performance of the QAM-FBMC system when using the optimized DPSS-based (DPSSb) prototype filters and compare the results with those obtained when using the prototype filter Case C proposed in [20] and Type I proposed in [13].

The performance of the prototype filters was evaluated through the bit error rate (BER) over Additive White Gaussian Noise (AWGN) channel and also over the pedestrian channel, defined by 3GPP [49]. The presented results are obtained by averaging over different channel instantaneous realizations. The performance evaluation was performed over different modulation levels: 4-QAM, 16-QAM and, 64-QAM.

In order to enhance the overall system performance, the iterative interference cancellation (IIC) [16], [18] was applied

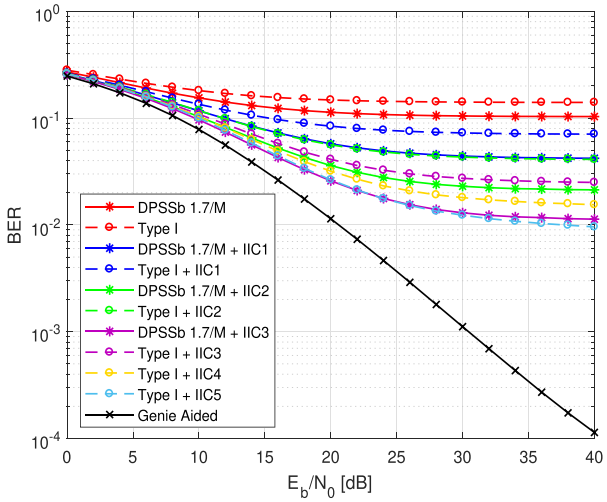


**FIGURE 11.** BER performance of QAM-FBMC system with 64QAM modulation, DPSSb 1.7/*M* filter and Type I [13] filter over pedestrian channel.

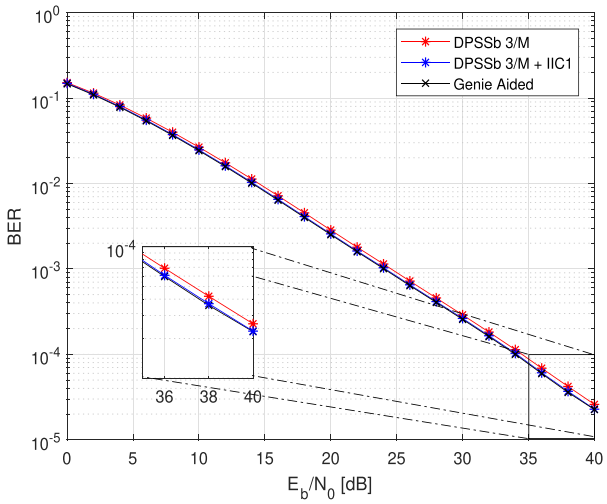


**FIGURE 12.** BER performance of QAM-FBMC system with 4QAM modulation, DPSSb 3/M filter over pedestrian channel.

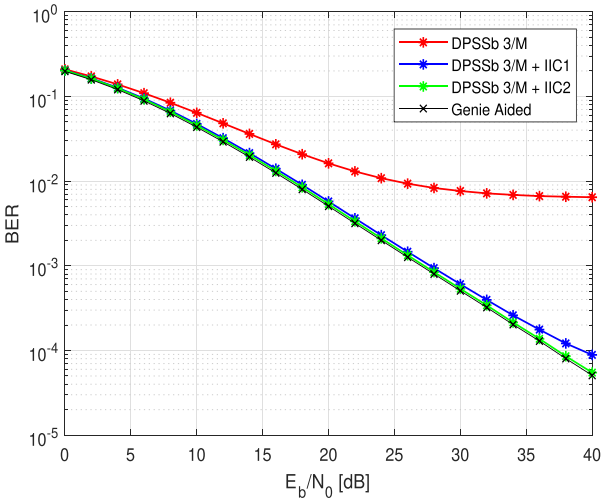


**FIGURE 13.** BER performance of QAM-FBMC system with 16QAM modulation, DPSSb 3/M filter over pedestrian channel.

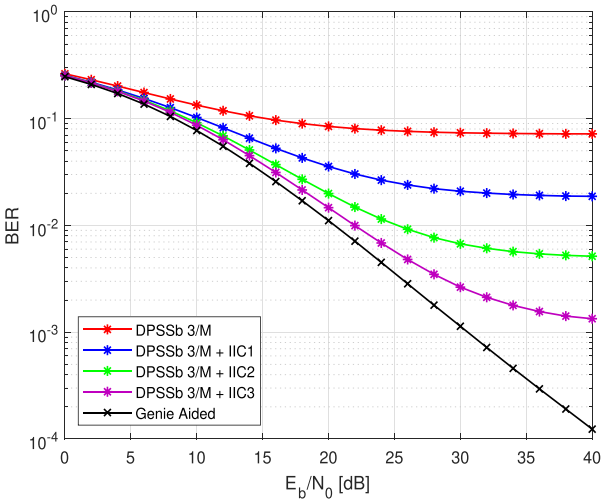


**FIGURE 14.** BER performance of QAM-FBMC system with 64QAM modulation, DPSSb 3/M filter over pedestrian channel.

at the receiver. For the sake of clarity, we also present the Genie Aided performance where the interference is assumed to be perfectly known at the receiver.

In Figs. 7 and 8, we present the BER performance of QAM-FBMC system over AWGN channel with 4-QAM and 16-QAM modulations respectively. We compare the results using DPSSb 1.7/*M* optimized filter with the results of Type I filter. In the case of 4-QAM modulation, the system performance can be significantly improved by the use of the optimized filter. However, with just one IIC iteration it is possible to achieve the same performance for both filters, which is the same as the Genie Aided. Even observing a significant degradation in the performance for 16-QAM modulation compared to the 4-QAM modulation, the proposed filter outperforms the Type I filter. In this case, applying the IIC technique, even with two IIC iterations, the proposed DPSSb 1.7/*M* outperforms the Type I filter.

The QAM-FBMC system was also evaluated over pedestrian channel. Figs. 9, 10, and 11 compare the performance of DPSSb 1.7/*M* and Type I filters when using 4, 16, and 64-QAM modulation respectively. In the case of 4-QAM modulation, even without using IIC technique, the DPSSb 1.7/*M* performance is very close to that of Genie Aided, whereas for Type I one IIC iteration is necessary to achieve the same performance.

Considering 16-QAM and 64-QAM modulation, we can observe an overall system degradation as expected. Once again the optimized filter outperforms the Type I filter and achieve the Genie Aided performance with 16-QAM modulation by performing 3 IIC iterations. Although for 64-QAM modulation the system suffers from high degradation, we can still confirm the superiority of the DPSSb 1.7/*M* filter, since

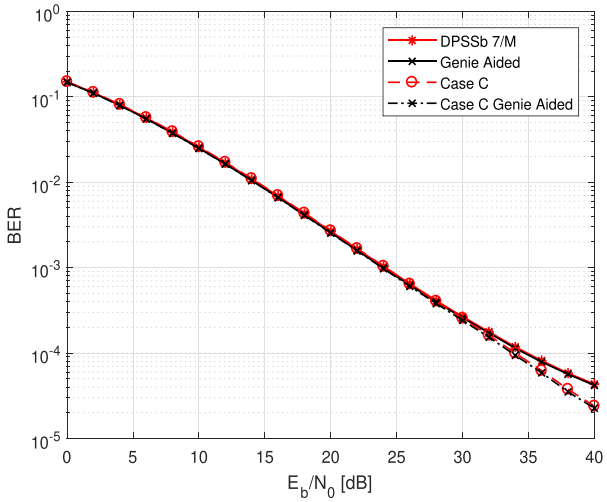


**FIGURE 15.** BER performance of QAM-FBMC system with 4QAM modulation, DPSSb 7/*M* filter and Case C [20] filter over pedestrian channel.

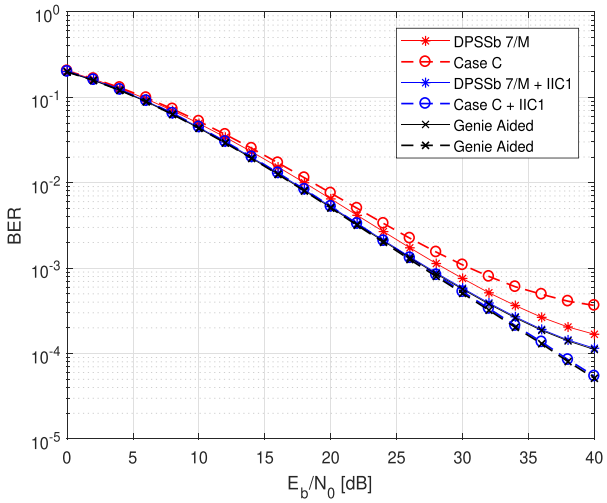


**FIGURE 16.** BER performance of QAM-FBMC system with 16QAM modulation, DPSSb 7/*M* filter and Case C [20] filter over pedestrian channel.

it achieves almost the same performance of Type I after 5 IIC iterations but with just 3 iterations.

As we did not find in the literature a prototype filter with approximately the same bandwidth to make a fair comparison to the DPSSb $3/M$, we present its performance in Figs. 12, 13, and 14 compared to the Genie Aided performance in the cases of 4-QAM, 16-QAM, and 64-QAM modulation respectively.

As we can see, for 4-QAM modulation we achieve the same performance as the Genie Aided, even without IIC. The Genie-Aided performance is achieved after 3 IIC iterations when the 16-QAM modulation is applied. In the case of 64-QAM modulation, the improvement obtained with our proposed DPSSb filter applied in tandem with IIC is significant.

For the comparison to the Case C filter, we have optimized a prototype filter DPSSb with bandwidth $B = 7/M$. We present, in Figs. 15, 16, and 17, the system performance

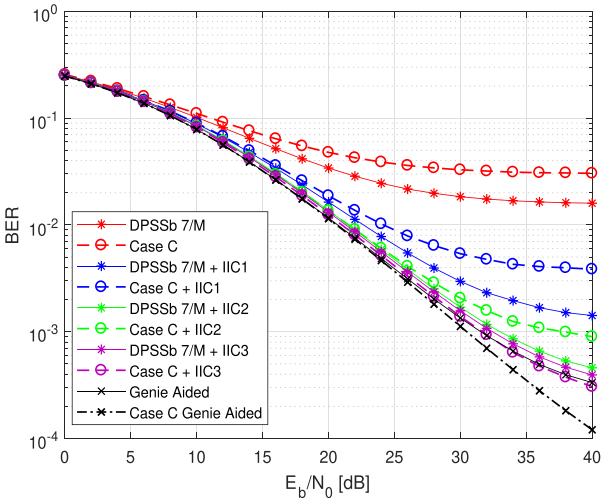


**FIGURE 17.** BER performance of QAM-FBMC system with 64QAM modulation, DPSSb 7/*M* filter and Case C [20] filter over pedestrian channel.

when applying 4-QAM, 16-QAM, and 64-QAM modulations, respectively.

In the case of 4-QAM modulation, the Genie-Aided performance is achieved even without IIC. Besides, both filters have the same performance until approximately 34dB of $E_b/N_0$. After that, the performances are slightly different. One IIC iteration is needed for achieving the same performance of Genie Aided in the case of 16-QAM modulation for both filters. However, without IIC the optimized filter outperforms the Case C filter. Once again we can notice a slight difference between the performances for $E_b/N_0$ greater than 34dB. In the case of 64-QAM modulation, the overall system performance deteriorates. Despite that, DPSSb $7/M$ filter achieves better results when compared with the Case C filter, until three IIC iterations, when they have very similar performance.

## VII. CONCLUSION

In this paper, we propose a novel method for the design of prototype filters for QAM-FBMC systems which are based on DPSS. We consider the spectral confinement through the band-time parameter of DPSS and minimize the intrinsic interference coefficients of the QAM-FBMC system. As a result, the obtained filters achieve smaller ISI than the competitors found in the literature. Furthermore, our proposed design shows to be flexible considering their adjustable parameters as bandwidth, overlapping factor, and filter length.

The performance of the proposed DSSSb filters was evaluated through the BER of the system and compared to known filters, such as Case C and Type I, which are strong competitors among the state of the art. We consider different modulation levels, AWGN, and pedestrian channels, and for all the considered scenarios the DPSSb-optimized filters outperform the competition, with and without interference cancellation.

## REFERENCES


[1] G. P. Fettweis and E. Matus, "Scalable 5G MPSoC architecture," in *Proc. 51st Asilomar Conf. Signals, Syst., Comput.*, Oct. 2017, pp. 613–618.

[2] S. E. Elayoubi, M. Fallgren, P. Spapis, G. Zimmermann, and D. Martín-Sacrist, "5G service requirements and operational use cases: Analysis and METIS II vision," in *Proc. Eur. Conf. Netw. Commun. (EuCNC)*, 2016, pp. 158–162.

[3] A. Gupta and R. K. Jha, "A survey of 5G network: Architecture and emerging technologies," *IEEE Access*, vol. 3, pp. 1206–1232, 2014.

[4] M. Bellanger, D. Le Ruyet, D. Roviras, M. Terré, and J. Nossek, "FBMC physical layer: A primer," *Phydyas*, vol. 25, pp. 7–10, Jan. 2010.

[5] R. Nissel, S. Schwarz, and M. Rupp, "Filter bank multicarrier modulation schemes for future mobile communications," *IEEE J. Sel. Areas Commun.*, vol. 35, no. 8, pp. 1768–1782, Aug. 2017.

[6] R. Zakaria, D. Le Ruyet, and M. Bellanger, "Maximum likelihood detection in spatial multiplexing with FBMC," in *Proc. Eur. Wireless Conf. (EW)*, 2010, pp. 1038–1041.

[7] M. Renfors, T. Ihalainen, and T. H. Stitz, "A block-alamouti scheme for filter bank based multicarrier transmission," in *Proc. Eur. Wireless Conf. (EW)*, 2010, pp. 1031–1037.

[8] B. Le Floch, M. Alard, and C. Berrou, "Coded orthogonal frequency division multiplex [TV broadcasting]," *Proc. IEEE*, vol. 83, no. 6, pp. 982–996, Jun. 1995.

[9] A. Vahlin and N. Holte, "Optimal finite duration pulses for OFDM," *IEEE Trans. Commun.*, vol. 44, no. 1, pp. 10–14, Jan. 1996.

[10] W. Kozek and A. F. Molisch, "Nonorthogonal pulseshapes for multicarrier communications in doubly dispersive channels," *IEEE J. Sel. Areas Commun.*, vol. 16, no. 8, pp. 1579–1589, Oct. 1998.

[11] T. Strohmer and S. Beaver, "Optimal OFDM design for time-frequency dispersive channels," *IEEE Trans. Commun.*, vol. 51, no. 7, pp. 1111–1122, Jul. 2003.

[12] R. Zakaria and D. Le Ruyet, "Intrinsic interference reduction in a filter bank-based multicarrier using QAM modulation," *Phys. Commun.*, vol. 11, pp. 15–24, Jun. 2014.

[13] Y. H. Yun, C. Kim, K. Kim, Z. Ho, B. Lee, and J.-Y. Seol, "A new waveform enabling enhanced QAM-FBMC systems," in *Proc. 16th Int. Workshop Signal Process. Adv. Wireless Commun. (SPAWC)*, 2015, pp. 116–120.

[14] H. Nam, M. Choi, S. Han, C. Kim, S. Choi, and D. Hong, "A new filter-bank multicarrier system with two prototype filters for QAM symbols transmission and reception," *IEEE Trans. Wireless Commun.*, vol. 15, no. 9, pp. 5998–6009, Sep. 2016.

[15] C. Kim, K. Kim, Y. H. Yun, Z. Ho, and B. Lee, "QAM-FBMC: A new multi-carrier system for post-OFDM wireless communications," in *Proc. Global Commun. Conf. (GLOBECOM)*, 2015, pp. 1–6.

[16] R. Zakaria, D. Le Ruyet, and Y. Medjahdi, "On ISI cancellation in MIMO-ML detection using FBMC/QAM modulation," in *Proc. Int. Symp. Wireless Commun. Syst. (ISWCS)*, Aug. 2012, pp. 949–953.

[17] H. Han, H. Kim, N. Kim, and H. Park, "An enhanced QAM-FBMC scheme with interference mitigation," *IEEE Commun. Lett.*, vol. 20, no. 11, pp. 2237–2240, Nov. 2016.

[18] S. Mahama, Y. J. Harbi, A. G. Burr, and D. Grace, "Iterative interference cancellation in FBMC-QAM systems," in *Proc. Wireless Commun. Netw. Conf. (WCNC)*, 2019, pp. 1–5.

[19] H. Han, G. Kwon, and H. Park, "MMSE-interference canceling receiver for QAM-FBMC systems," *IEEE Commun. Lett.*, vol. 24, no. 11, pp. 2589–2593, Nov. 2020.

[20] H. Kim, H. Han, and H. Park, "Waveform design for QAM-FBMC systems," in *Proc. IEEE 18th Int. Workshop Signal Process. Adv. Wireless Commun. (SPAWC)*, Jul. 2017, pp. 1–5.

[21] H. Han and H. Park, "Design on the waveform for QAM-FBMC system in the presence of residual CFO," in *Proc. 16th IEEE Annu. Consum. Commun. Netw. Conf. (CCNC)*, Jan. 2019, pp. 1–2.

[22] H. Han, N. Kim, and H. Park, "Design of QAM-FBMC waveforms considering MMSE receiver," *IEEE Commun. Lett.*, vol. 24, no. 1, pp. 131–135, Jan. 2020.

[23] I. Galdino Andrade, R. Zakaria, D. Le Ruyet, and M. L. R. de Campos, "Short-filter design for intrinsic interference reduction in QAM-FBMC modulation," *IEEE Commun. Lett.*, vol. 24, no. 7, pp. 1487–1491, Jul. 2020.

[24] D. Slepian and H. O. Pollak, "Prolate spheroidal wave functions, Fourier analysis and uncertainty-I," *Bell Syst. Tech. J.*, vol. 40, no. 1, pp. 43–63, 1961.

[25] H. J. Landau and H. O. Pollak, "Prolate spheroidal wave functions, Fourier analysis and uncertainty-II," *Wiley Library-Bell Syst. Tech. J.*, vol. 40, no. 1, pp. 65–84, 1961.

[26] D. B. Percival, *Spectral Analysis for Physics Application*. Cambridge, U.K.: Cambridge Univ. Press, 1993.

[27] I. C. Moore and M. Cada, "Prolate spheroidal wave functions, an introduction to the Slepian series and its properties," *Appl. Comput. Harmon. Anal.*, vol. 16, no. 3, pp. 208–230, 2004.

[28] J. Shen, "Highly accurate pseudospectral approximations of the prolate spheroidal wave equation for any bandwidth parameter and zonal wavenumber," *J. Sci. Comput.*, vol. 71, no. 2, pp. 804–821, May 2017.

[29] L. Wang, "A review of prolate spheroidal wave functions from the perspective of spectral methods," *J. Math. Study*, vol. 50, no. 2, pp. 101–143, Jun. 2017.

[30] M. Boulsane, N. Bourguiba, and A. Karoui, "Discrete prolate spheroidal wave functions: Further spectral analysis and some related applications," *J. Sci. Comput.*, vol. 82, no. 3, pp. 1–19, Mar. 2020.

[31] A. Tkacenko, P. P. Vaidyanathan, and T. Q. Nguyen, "On the eigenfilter design method and its applications: A tutorial," *IEEE Trans. Circuits Syst. II, Analog Digit. Signal Process.*, vol. 50, no. 9, pp. 497–517, Sep. 2003.

[32] J. Mathews, J. Breakall, and G. Karawas, "The discrete prolate spheroidal filter as a digital signal processing tool," *IEEE Trans. Acoust., Speech, Signal Process.*, vol. ASSP-33, no. 6, pp. 1471–1478, Dec. 1985.

[33] M. A. Davenport and M. B. Wakin, "Compressive sensing of analog signals using discrete prolate spheroidal sequences," *Appl. Comput. Harmon. Anal.*, vol. 33, no. 3, pp. 438–472, Nov. 2012.

[34] F. Yin, C. Debes, and A. M. Zoubir, "Parametric waveform design using discrete prolate spheroidal sequences for enhanced detection of extended targets," *IEEE Trans. Signal Process.*, vol. 60, no. 9, pp. 4525–4536, Sep. 2012.

[35] Z. Zhu and M. B. Wakin, "Wall clutter mitigation and target detection using discrete prolate spheroidal sequences," in *Proc. 3rd Int. Workshop Compressed Sens. Theory Appl. Radar, Sonar Remote Sens. (CoSeRa)*, Jun. 2015, pp. 41–45.

[36] S. Soman and M. Cada, "Design and simulation of a linear prolate filter for a baseband receiver," *J. Inf. Technol. Softw. Eng.*, vol. 7, no. 1, p. 197, 2017.

[37] A. Triana, D. Pastor, and M. Varon, "Code division multiplexing applied to FBG sensing networks: FBG sensors designed as discrete prolate spheroidal sequences (DPSS-FBG Sensors)," *J. Lightw. Technol.*, vol. 35, no. 14, pp. 2880–2886, Jul. 15, 2017.

[38] B. P. Day, A. Evers, and D. E. Hack, "Multipath Suppression for Continuous Wave Radar via Slepian Sequences," *IEEE Trans. Signal Process.*, vol. 68, pp. 548–557, 2020.

[39] A. Ron and Z. Shen, "Frames and stable bases for shift-invariant subspaces of $L_2$ ($\mathbb{R}$d)," *Can. J. Math.*, vol. 47, no. 5, pp. 1051–1094, 1995.

[40] P. M. Woodward, *Probablity Information Theory, With Applications to Radar*. London, U.K.: Pergamon, 1953.

[41] D. Slepian, "Some comments on Fourier analysis, uncertainty and modeling," *SIAM Rev.*, vol. 25, no. 3, pp. 379–393, Jul. 1983.

[42] C. Flammer, *Spheroidal Wave Functions, A Stanford Research Inst*. Stanford, CA, USA: Stanford Univ. Press, 1957.

[43] A. Osipov, V. Rokhlin, and H. Xiao, *Prolate Spheroidal Wave Functions Order Zero*, vol. 187. New York, NY, USA: Springer, 2013.

[44] D. Slepian, "Prolate spheroidal wave functions, Fourier analysis, and uncertainty-V: The discrete case," *Bell Syst. Tech. J.*, vol. 57, no. 5, pp. 1371–1430, May 1978.

[45] T. Zemen and C. F. Mecklenbrauker, "Time-variant channel estimation using discrete prolate spheroidal sequences," *IEEE Trans. Signal Process.*, vol. 53, no. 9, pp. 3597–3607, Sep. 2005.

[46] J. Kaiser and R. Schafer, "On the use of the $I_0$-sinh window for spectrum analysis," *IEEE Trans. Acoust., Speech, Signal Process.*, vol. ASSP-28, no. 1, pp. 105–107, Aug. 1980.

[47] A. Sahin, I. Guvenc, and H. Arslan, "A survey on multicarrier communications: Prototype filters, lattice structures, and implementation aspects," *IEEE Commun. Surveys Tuts.*, vol. 16, no. 3, pp. 1312–1338, 3rd Quart., 2014.

[48] S. Boyd and L. Vandenberghe, *Convex Optimization*. Cambridge, U.K.: Cambridge Univ. press, 2004.

[49] *Base Station (BS) Radio Transmission and Reception*, document TS 36.104, 3GPP, 2010. [Online]. Available: https://portal.3gpp.org/desktopmodules/Specifications/SpecificationDetails.aspx?specificationId=2412

**IANDRA GALDINO** received the engineering degree in telecommunications engineering from Fluminense Federal University (UFF), Niterói, Rio de Janeiro, Brazil, in 2015, the M.Sc. degree in electrical engineering from the Federal University of Rio de Janeiro (COPPE/UFRJ), in 2017, and the joint Ph.D. degree in electrical engineering from the COPPE/UFRJ and the CEDRIC/LAETITIA Research Laboratory, Conservatoire National des Arts et Métiers (CNAM), Paris, France.

She is currently a Postdoctoral Fellow with the MidiaCom Laboratory, Institute of Computing, UFF. Her research interests include communication systems, multicarrier waveforms, and signal processing. Her current research interest includes waveform design for post 5G systems.

**ROSTOM ZAKARIA** received the engineering degree in electronics from the University of Science and Technology Houari Boumediene, Algiers, Algeria, in 2007, the M.Sc. degree from the University of Paris-Est Marne-La-Vallée, France, in 2008, and the Ph.D. degree from the CEDRIC/LAETITIA Research Laboratory, Conservatoire National des Arts et Métiers (CNAM), Paris, in 2012.

From 2012 to 2018, he has been a temporary Assistant Professor and a Researcher with CNAM. In 2016, he spent one month as a Visiting Research Fellow at the Department of Electrical and Computer Engineering, Seoul National University (SNU), Seoul, South Korea. Since 2018, he has been a Freelance Research Consultant and a Lecturer, where he worked for the HUAWEI Paris Research Center during two years and provided 11 patent ideas on beyond 5G waveforms. His main research interests include in general to digital communications and signal processing, including in particular interference cancellation techniques, filtered multicarrier modulations, and waveform design for next generation wireless communications.

Dr. Zakaria was one of the recipients of the Timely Incentive Team Award and the President Award—the Best Technology Innovation Award from the HUAWEI Paris Research Center, in 2019 and 2020, respectively.

**DIDIER LE RUYET** (Senior Member, IEEE) received the Eng. and Ph.D. degrees from the Conservatoire National des Arts et Métiers (CNAM), Paris, in 1994 and 2001, respectively, and the "Habilitation à Diriger des Recherches" degree from Sorbonne Paris Nord University, in 2009.

From 1988 to 1996, he was a Senior Member of the Technical Staff at SAGEM Defence and Telecommunication, France. He joined the Signal and Systems Laboratory, CNAM, as a Research Assistant, in 1996. From 2002 to 2010, he was an Assistant Professor at CNAM, where he has been a Full Professor with the CEDRIC Research Laboratory, since 2010. From 2016 to 2019, he was the Deputy Director of the CEDRIC. He has published about 200 papers in refereed journals and conference proceedings and has published five books in the area of digital communication. He has been involved in several national and European projects dealing with multicarrier transmission techniques and multiantenna transmission. His main research interests include the areas of digital communications and signal processing including channel coding, detection and estimation algorithms, filter-bank-based multicarrier communication, and multiantenna transmission.

Dr. Le Ruyet served as a Technical Program Committee Member for major IEEE ComSoc and VTS conferences, and as the General Chair for the Ninth Edition of ISWCS'2012 Conference and the Co-Chair for the ISWCS 2013 and 2019 edition.

**MARCELLO L. R. DE CAMPOS** (Senior Member, IEEE) was born in Niterói, Brazil, in 1968. He received the engineering degree *(cum laude)* from the Federal University of Rio de Janeiro (UFRJ), Rio de Janeiro, Brazil, in 1990, the M.Sc. degree from COPPE/UFRJ, in 1991, and the Ph.D. degree from the University of Victoria, Victoria, BC, Canada, in 1995, all in electrical engineering.

In 1996, he was a Postdoctoral Fellow with the Department of Electronics, School of Engineering, UFRJ, and with the Program of Electrical Engineering, COPPE/UFRJ. From January 1997 to May 1998, he was an Associate Professor with the Department of Electrical Engineering (DE/3), Military Institute of Engineering (IME), Rio de Janeiro. He is currently the Deputy Director for Academic Affairs at the COPPE/UFRJ and a Professor of the Program of Electrical Engineering, where he has also served as the Department Vice-Chair and the Chair, in 2004 and 2005, respectively. As a Visiting Scholar, he has spent small sabbatical periods at the Laboratory for Telecommunications Technology, Helsinki University of Technology, Espoo, Finland; the Centre for Wireless Communications, University of Oulu, Oulu, Finland; the University Graduate Center, University of Oslo, Oslo, Norway; Aalto University, Helsinki, Finland; and the Norwegian University of Science and Technology, Trondheim, Norway. He is a CNPq productivity researcher level 1-D, his curriculum vitae can be retrieved from his website (http://lattes.cnpq.br/2402401592333107), and he is associated with the Signals, Multimedia, and Signal Processing Laboratory, COPPE/UFRJ. He has taught over 150 courses on mobile communications in 15 countries, and managed numerous research and development projects in signal processing and communications for technology companies in Brazil and abroad. His research interests include adaptive signal processing in general and its application to distributed networks in particular, adaptive beamforming, statistical signal processing, statistical and machine learning, optimization, signal processing for communications, underwater, mobile and wireless communications, and MIMO systems.

Prof. De Campos served as the IEEE Communications Society Regional Director for Latin America, in 2000 and 2001; the Local-Arrangements Co-Chair for GLOBECOM'99; the Finance Chair for SPAWC 2008; the Plenary Chair for ISCAS 2011; and the Technical Co-Chair for the 2013 Brazilian Telecommunications Symposium. He founded and was the Chair of the IEEE Signal Processing Society Rio de Janeiro Chapter for four years.